Supplementary Material

Structural bases for the broad specificity of a new family of amino acid racemases

Akbar Espaillat, Cesar Carrasco-López, Noelia Bernardo-Garcia, Natalia Pietrosemoli, Lisandro H. Otero, Laura Alvarez, Miguel A. de Pedro, Florencio Pazos, Brigid M. Davis, Matthew K. Waldor, Juan A. Hermoso and Felipe Cava

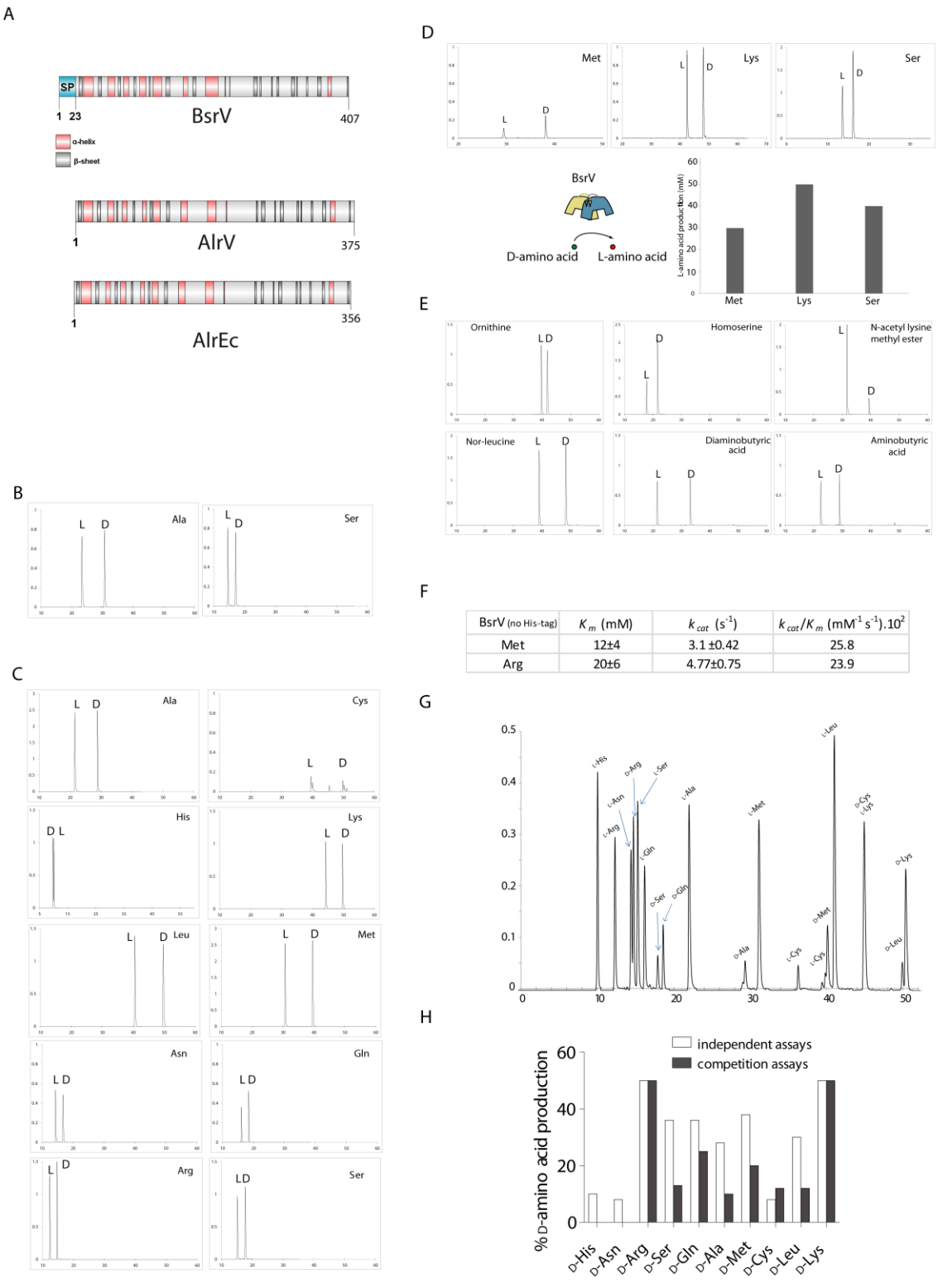

BsrV (no His-tag)	K_m (mM)	k_{cat} (s^{-1})	k_{cat}/K_m ($mM^{-1}\ s^{-1}$).10^2
Met	12±4	3.1 ±0.42	25.8
Arg	20±6	4.77±0.75	23.9

Supplementary Figure S1. Biochemical comparison of AlrV and BsrV from *V. cholerae.* (A) Prediction of protein domains for BsrV, AlrV and Alr_{Ec}. Representation of protein features obtained with UNIPROT. In pink is shown the α-helix, in grey the β-sheet and in blue the signal peptide (predicted with the online tool PSIPRED. (B-E) Racemization of amino acids by *V. cholerae´s* AlrV and BsrV. Chromatograms show HPLC analysis of Marfey's derivatized amino acids after *in vitro* racemase reactions; (B) AlrV and (C) BsrV activity on natural (proteinogenic) amino acids. (D) Reverse reaction starting from D-amino acids in BsrV. (E) BsrV activity on non-proteinogenic amino acids. (F) Kinetic values with Met and Arg of mature BsrV without His-tag. Note that kinetic analyses for representative amino acids yielded the same result using tagged (Fig. 1) and untagged protein. (G) Chromatograms of the derivatized products of a 5 minutes reaction containing BsrV and all natural racemizable amino acids. (H) Yield of DAA produced by BsrV in independent (white bars) and competition reactions (black bars).

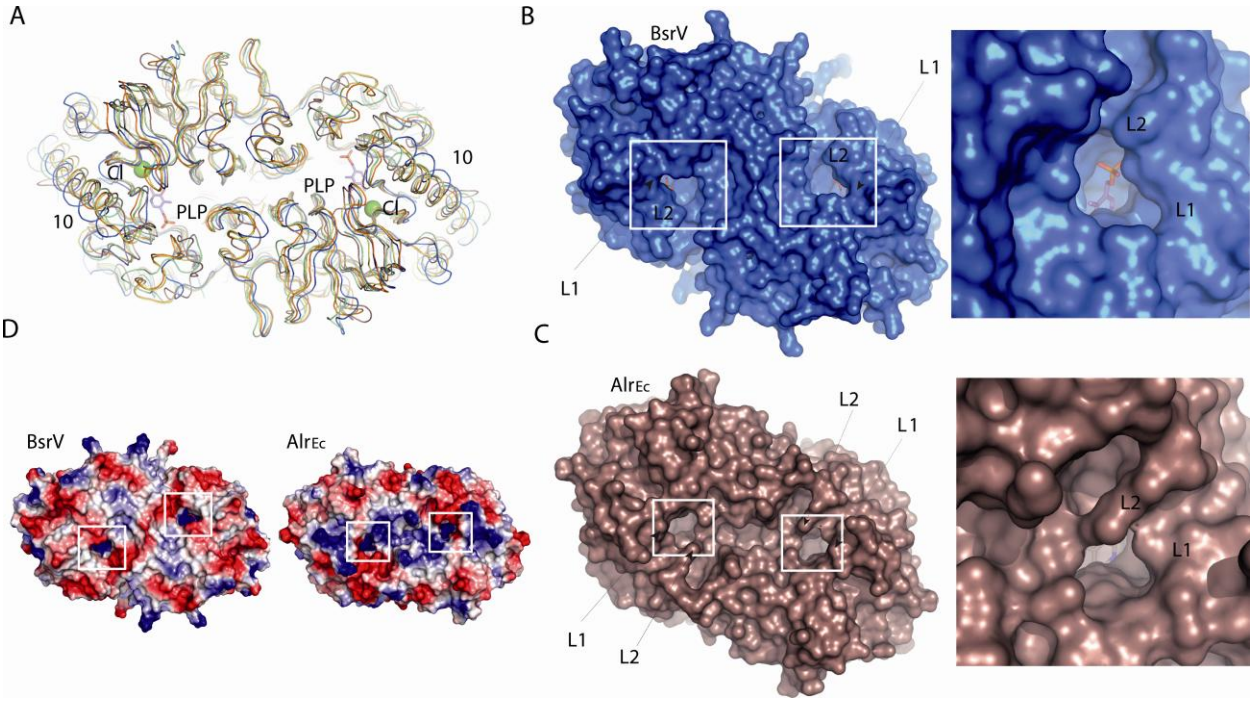

Supplementary Figure S2. Structural comparison of multispecific BsrV and monospecific racemases. (A) Ribbon representation of BsrV (blue) superimposed on Ser racemase from *E. faecalis* (PDB code 4ECL) colored in green, Ala racemase from *B. anthracis* (PDB code 2VD8) colored in yellow, Ala racemase from *G. stearothermophilus* (PDB code 1NIU) colored in orange and Ala racemase from *E. coli* (PDB code 2RJG) colored in brown. Cl^- ion and PLP (pyridoxal phosphate) from BsrV are depicted as spheres and sticks respectively. (B) Molecular surface of BsrV with L1 and L2 loops labeled. Active sites are highlighted in white boxes. Right, zoom of the active site with PLP in sticks. (C) Molecular surface of *E. coli* Ala racemase (Alr_{Ec}) with L1 and L2 loops labeled. Active sites are highlighted in white boxes. Right, zoom of the active site with PLP in sticks. Panels B and C keep the same orientation. (D)

Electrostatic Potential molecular surface for BsrV and Alr_{Ec}. Acidic regions are colored in red and basic regions in blue. Active sites are highlighted in white boxes.

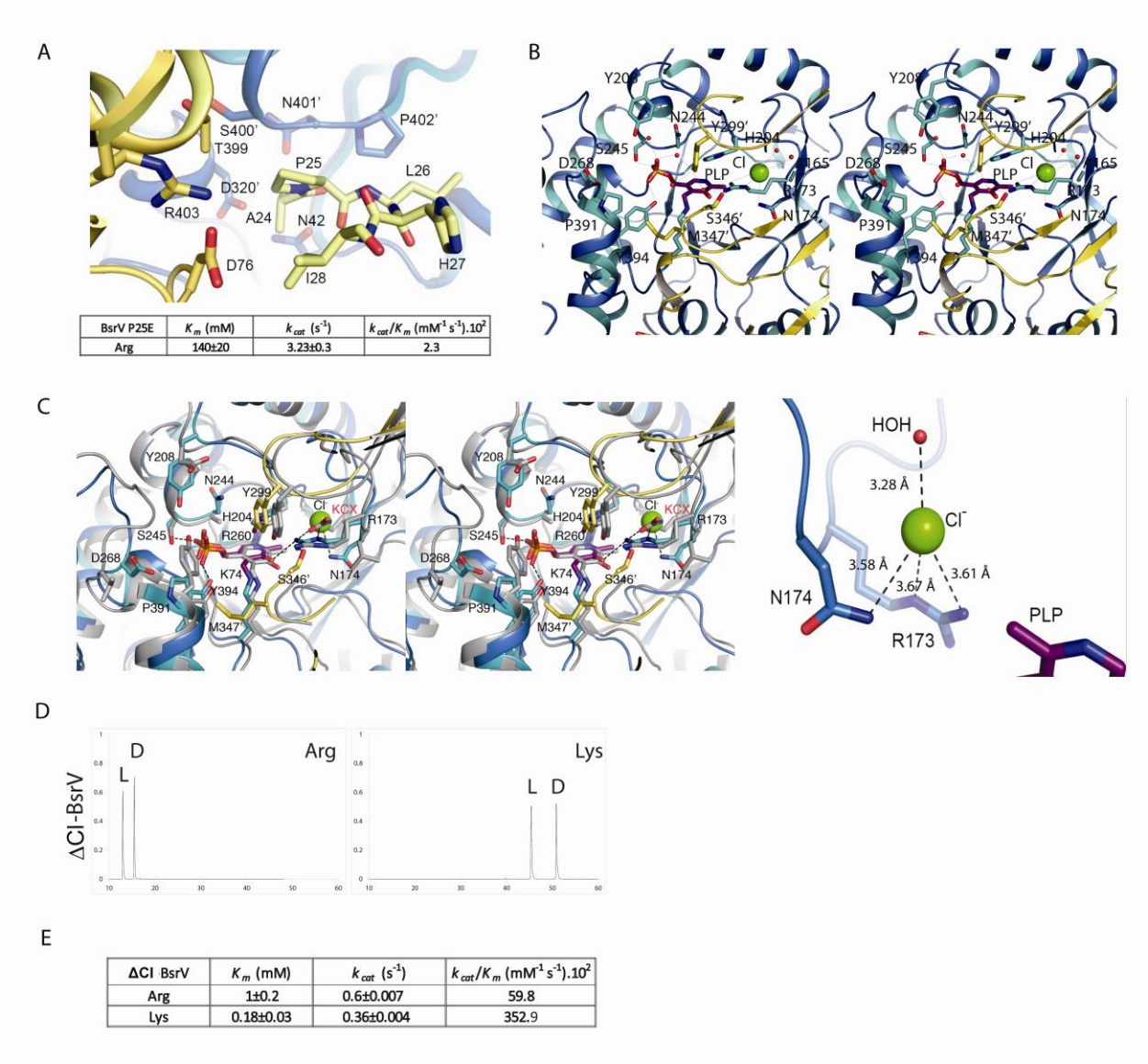

BsrV P25E	K_m (mM)	k_{cat} (s^{-1})	k_{cat}/K_m ($mM^{-1} s^{-1}$).10^2
Arg	140±20	3.23±0.3	2.3

ΔCl BsrV	K_m (mM)	k_{cat} (s^{-1})	k_{cat}/K_m ($mM^{-1} s^{-1}$).10^2
Arg	1±0.2	0.6±0.007	59.8
Lys	0.18±0.03	0.36±0.004	352.9

Supplementary Figure S3. BsrV and ΔCl-BsrV active site structure and kinetic parameters. Related to Figure 3. (A) Structural environment of Pro25 as part of the N-terminal extension in BsrV. Monomers of BsrV are colored as in Figure 2A. Relevant residues, involved in Pro25 packing, are represented as sticks. (B) Stereo view of the BsrV active site. Monomers of BsrV are colored as in Figure 2A. Relevant residues are

represented in sticks. PLP molecules are drawn in sticks. Cl^- ions and water molecules as green and red spheres respectively. (C) Left, Stereo view of the structural merge of Alr_{Ec} and BsrV active site. In grey is represented the structure of Alr_{Ec} and in blue BsrV. Relevant residues of the BsrV catalytic machinery (blue sticks) are labeled. The equivalent residues from Alr_{Ec} are represented as grey sticks and its N-carboxylated lysine is labeled in red. The green sphere represents BsrV´s chloride atom. PLP molecules are drawn in sticks. Right, stabilization of the chloride ion is shown and distances are labeled. Analysis of the Cl coordination using the Cambridge Crystallographic Data Base (http://webcsd.ccdc.cam.ac.uk/) reveals that the average distances for Cl-N and Cl-O are 3.29 (± 0.5) Å and 3.19 (± 0.3) Å respectively. A search for all the deposited protein structures presenting a halogen coordinated by Arg and Asn residues was done by using Relibase (http://www.ccdc.cam.ac.uk/Solutions/FreeSoftware/Pages/Relibase.aspx). In all the 38 entries in PDB presenting such geometry the halogen corresponded to a chloride ion. (D) Representative chromatograms of Marfey's derivatized amino acids (Arg and Lys) after in vitro reaction with apo-BsrV for 90min. (E) Kinetic parameters (K_m, k_{cat} and k_{cat}/K_m) for various amounts (1.25-60 mM) of Arg and Lys were calculated using data obtained with 0.47 □M purified apo-BsrV racemase. The enzymatic reactions were measured as described in Materials and Methods. Results in panels B are means ± SD of triplicates from two independent experiments.

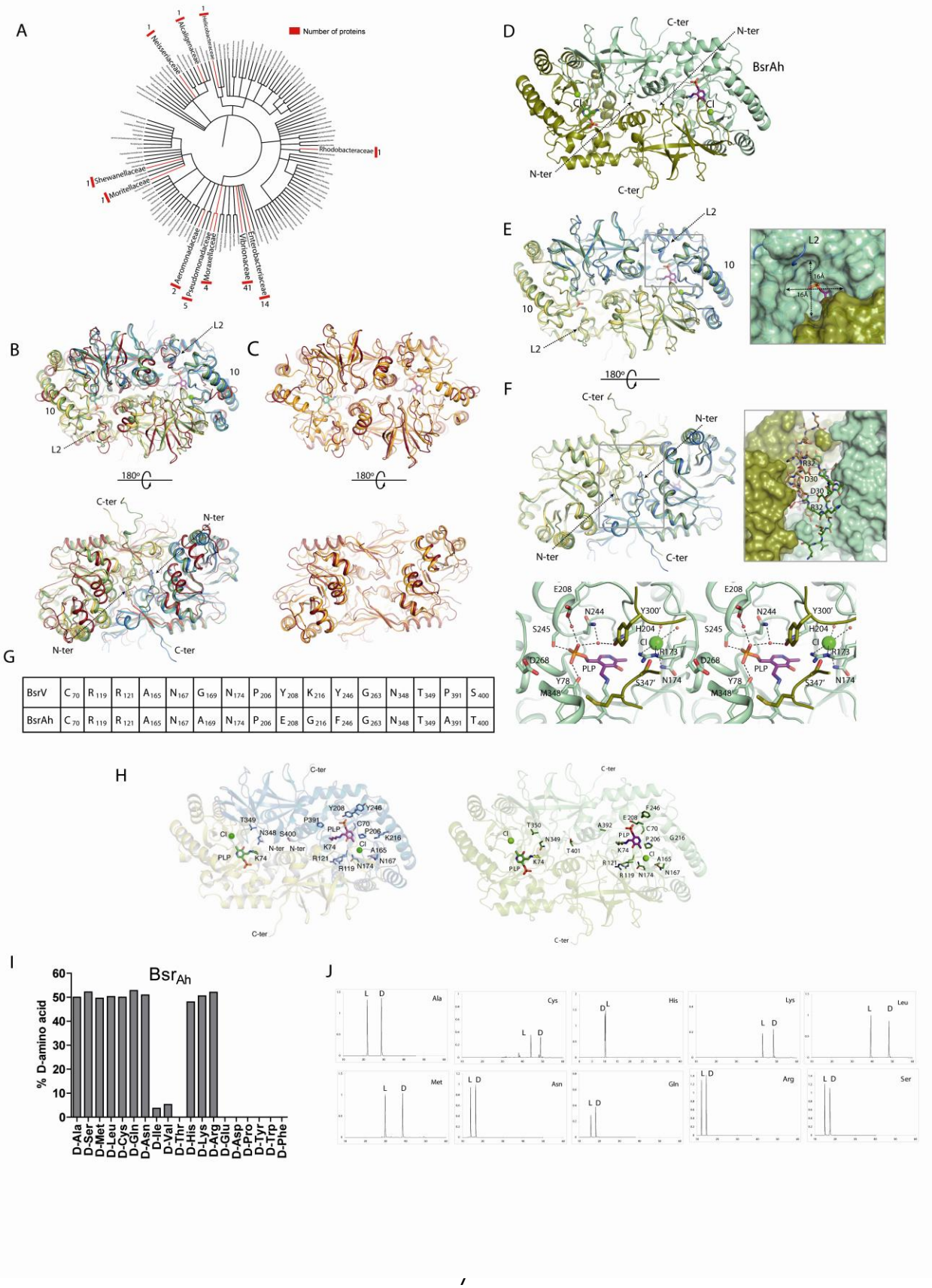
A
Number of proteins
Neisseriaceae
Alcaligenaceae
Rhodobacteraceae
Shewanellaceae
Moritellaceae
Aeromonadaceae
Pseudomonadaceae
Moraxellaceae
Vibrionaceae
Enterobacteriaceae
B
C
L2
180°
C-ter
N-ter
D
BsrAh
Cl
E
F
R32
D30
G
BsrV C70 R119 R121 A165 N167 G169 N174 P206 Y208 K216 Y246 G263 N348 T349 P391 S400
BsrAh C70 R119 R121 A165 N167 A169 N174 P206 E208 G216 F246 G263 N348 T349 A391 T400
H
PLP
I
BsrAh
% D-amino acid
D-Ala D-Ser D-Met D-Leu D-Cys D-Gln D-Asn D-Ile D-Val D-Thr D-His D-Lys D-Arg D-Glu D-Asp D-Pro D-Tyr D-Trp D-Phe
J
Ala
Cys
His
Lys
Leu
Met
Asn
Gln
Arg
Ser

Supplementary Figure S4. Identification of 16 residues that constitute the molecular footprint for BsrV multispecificity and experimental validation. (A) Phylogenetic tree of the families of 74 proteins identified, belonging to 37 different species. Red leaves correspond to protein families of the proteins in the dataset, the number of proteins belonging to the given family is also specified. (B) Structural superimposition of Alr_{Ah} (red cartoon) with BsrV (colored as in Fig. 2A) and Bsr_{Ah} (colored in different shades of green). Loop L2 and the α-helix α10, at the entry channel, are labeled. Chloride atoms are represented as spheres. PLP molecules are drawn in sticks. At the bottom, backside (180º rotation) of the dimer is shown. (C) Structural superimposition of Alr_{Ah} (red cartoon) with alanine racemase DadX from *Pseudomonas aeruginosa* (PDB code 1RCQ) (orange cartoon). PLP molecules are drawn in sticks. At the bottom, backside (180º rotation) of the dimer is shown. (D) Crystal structure of Bsr_{Ah} dimer with monomers depicted in different shades of green. PLP molecules are drawn in sticks and Cl^- ions as green spheres. (E) Structural superimposition of Bsr_{Ah} (colored as in panel D) with BsrV (colored as in panel B). Loop L2 and the α-helix α10, at the entry channel, are labeled. On the right box, differences in their active-site cavities are shown. Bsr_{Ah} molecular surface is colored as in panel A and BsrV is represented in blue cartoon. Dimensions at the entrance of Bsr_{Ah} cavity are shown by black arrows. (F) Backside (180º rotation) of the dimer. The Bsr_{Ah} N-terminal insertion is highlighted in the box. On the right, close-up view with the N-terminal insertion in sticks. At the bottom, stereoview of Bsr_{Ah} active site. Relevant residues and PLP are drawn in sticks, water molecules and Cl^- ions are drawn as red and green spheres, respectively. (G) Comparative analysis of BsrV and Bsr_{Ah} footprint residues. (H) Localization of the footprint residues in

BsrV (left) and Bsr_{Ah} (right) structural models. (I) Quantitative Bsr_{Ah} D-amino acid production spectra. (J) Chromatograms of racemizable amino acids by Bsr_{Ah}.

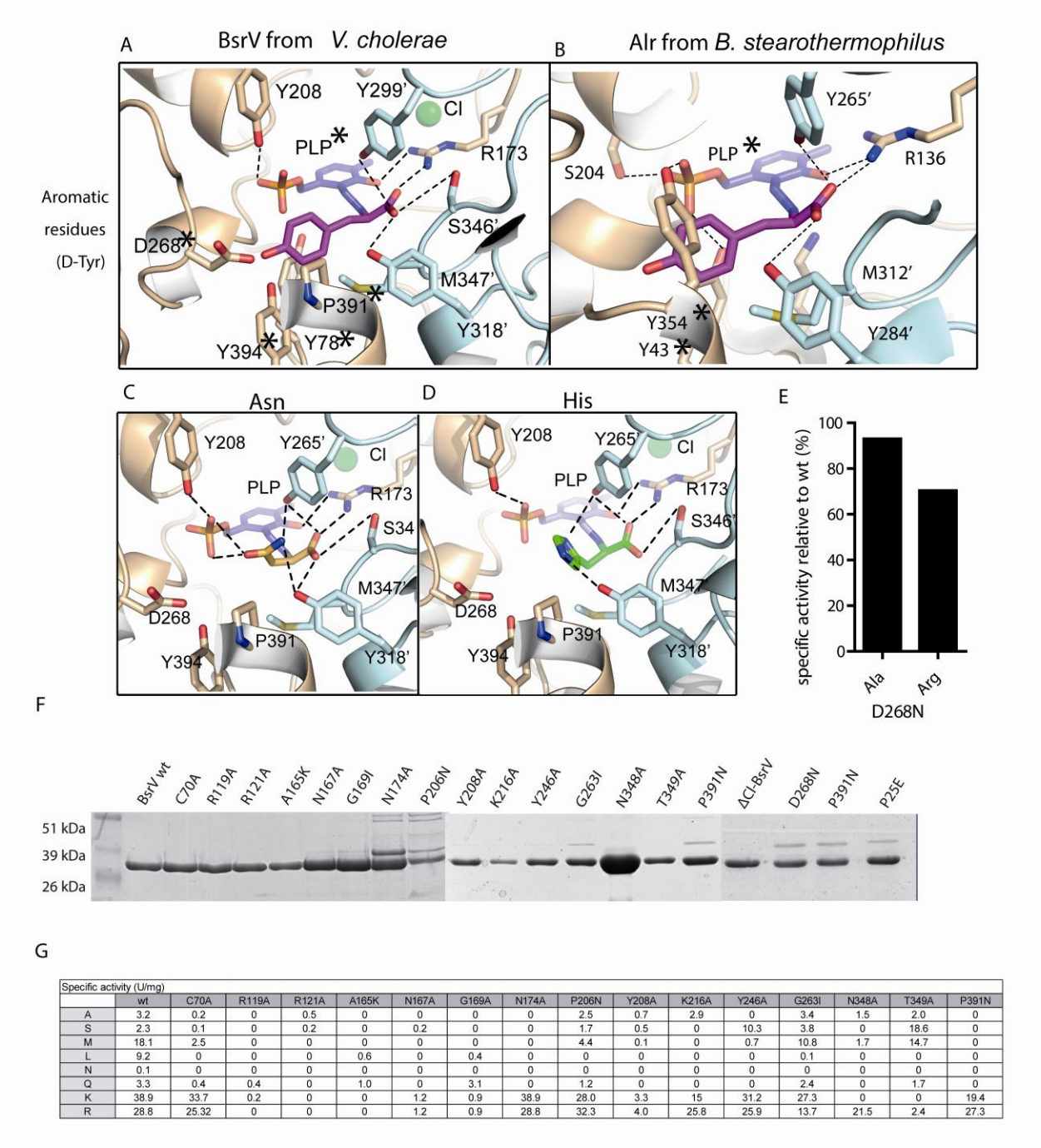

G

Specific activity (U/mg)																
	wt	C70A	R119A	R121A	A165K	N167A	G169A	N174A	P206N	Y208A	K216A	Y246A	G263I	N348A	T349A	P391N
A	3.2	0.2	0	0.5	0	0	0	0	2.5	0.7	2.9	0	3.4	1.5	2.0	0
S	2.3	0.1	0	0.2	0	0.2	0	0	1.7	0.5	0	10.3	3.8	0	18.6	0
M	18.1	2.5	0	0	0	0	0	0	4.4	0.1	0	0.7	10.8	1.7	14.7	0
L	9.2	0	0	0	0.6	0	0.4	0	0	0	0	0	0.1	0	0	0
N	0.1	0	0	0	0	0	0	0	0	0	0	0	0	0	0	0
Q	3.3	0.4	0.4	0	1.0	0	3.1	0	1.2	0	0	0	2.4	0	1.7	0
K	38.9	33.7	0.2	0	0	1.2	0.9	38.9	28.0	3.3	15	31.2	27.3	0	0	19.4
R	28.8	25.32	0	0	0	1.2	0.9	28.8	32.3	4.0	25.8	25.9	13.7	21.5	2.4	27.3

Supplementary Figure S5. DAA recognition by BsrV from *V. cholerae versus* Alr from *B. stearothermophilus*. (A) Docking model with the aromatic residue D-Tyr in BsrV (in purple sticks). (B) Docking model with the aromatic amino acid D-Tyr in Alr_{Bs} (in purple sticks). (C) Docking model with Asn in BsrV (in yellow sticks). (D) Docking model with

His in BsrV (in yellow sticks). (E) Specific activity of the BsrV D268N mutant relative to wt on Ala and Arg as representative amino acids of a non-charged and a positively charged amino acid. (F) SDS-PAGE analysis of purified proteins after Ni-NTA affinity chromatography purification. (G) Specific activity of 15 point mutants on BsrV's footprint residues.

Supplementary Table S1. Plasmids used in this study.

PLASMID	DESCRIPTION	REFERENCE
pET28b (+)	Kan^r, lacI. Expression of genes in *E. coli*, dependent on T7 phage RNA polymerase.	Novagen
pET28b AlrV	Kan^r. AlrV overexpression. 6His N-terminal fusion. (NdeI/EcoRI). DNA fragment (*V. cholerae*'s locus VC0372) amplified with FCP598 and FCP597 primers.	(Lam et al., 2009)
pET28b BsrV WT	Kan^r. BsrV WT overexpression with 6His C-terminal fusion. (NotI/EcoRI). DNA fragment (*V. cholerae*'s locus VC1312) amplified with FCP43 and FCP56 primers.	(Lam et al., 2009)
pET28b Alr_{Ah}	Kan^r. Alr_{Ah} overexpression with 6His C-terminal fusion. (NdeI/EcoRI). DNA fragment (*A. hydrofila*'s locus AHA1015) amplified with FCP108 and FCP109 primers.	This study
pET28b ΔCl-BsrV	Kan^r. BsrV R173N174/AA with C-terminal fusion of 6 histidines (NcoI/NotI). The mutation was introduced with FCP37 and FCP38 primers, replacing RN/AA in BsrV catalytic center.	This study
pET28b BsrV.tev.His	Kan^r. BsrV WT with Tev protease recognition site before the 6His C-terminal fusion (NcoI/NotI). DNA fragment amplified with FCP56 and FCP140 primers.	This study
pET28 BsrV P25E	Kan^r. BsrV P25E overexpression with 6His C-terminal fusion. (NcoI/NotI). The mutation was introduced with FCP63 and FCP64, replacing P/E in BsrV 25 position.	
pET28b BsrV C70A	Kan^r. BsrV C70A overexpression with 6His C-terminal fusion (NcoI/NotI). The mutation was introduced with FCP110 and FCP111 primers, replacing C/A in BsrV 70 position.	This study
pET28b BsrV R119A	Kan^r. BsrV R119A overexpression with 6His C-terminal fusion (NcoI/NotI). The mutation was introduced with FCP112 and FCP113 primers, replacing R/A in BsrV 119 position.	This study
pET28b BsrV R121A	Kan^r. BsrV R121A overexpression with 6His C-terminal fusion (NcoI/NotI). The mutation was introduced with FCP114 and FCP115 primers, replacing R/A in BsrV 121 position.	This study
pET28b BsrV A165K	Kan^r. BsrV A165K overexpression with 6His C-terminal fusion (NcoI/NotI). The mutation was introduced with FCP116 and FCP117 primers, replacing A/K in BsrV 165 position.	This study
pET28b BsrV N167A	Kan^r. BsrV N167A overexpression with 6His C-terminal fusion (NcoI/NotI). The mutation was introduced with FCP118 and FCP119 primers, replacing N/A in BsrV 167 position.	This study
pET28b BsrV G169I	Kan^r. BsrV G169I overexpression with 6His C-terminal fusion (NcoI/NotI). The mutation was introduced with FCP120 and FCP121 primers, replacing G/I in BsrV 169 position.	This study
pET28b BsrV N174A	Kan^r. BsrV N174A overexpression with 6His C-terminal fusion (NcoI/NotI). The mutation was introduced with FCP122 and FCP123	This study

	primers, replacing N/A in BsrV 174 position.	
pET28b BsrV P206N	Kan^r. BsrV P206N overexpression with 6His C-terminal fusion (NcoI/NotI). The mutation was introduced with FCP124 and FCP125 primers, replacing P/N in BsrV 206 position.	This study
pET28b BsrV Y208A	Kan^r. BsrV Y208A overexpression with 6His C-terminal fusion (NcoI/NotI). The mutation was introduced with FCP126 and FCP127 replacing Y/A in BsrV 208 position.	This study
pET28b BsrV K216A	Kan^r. BsrV K216A overexpression with 6His C-terminal fusion (NcoI/NotI). The mutation was introduced with FCP128 and FCP129 primers, replacing K/A in BsrV 216 position.	This study
pET28b BsrV Y246A	Kan^r. BsrV Y246A overexpression with 6His C-terminal fusion (NcoI/NotI). The mutation was introduced with FCP130 and FCP131 primers, replacing Y/A in BsrV 246 position.	This study
pET28b BsrV G263I	Kan^r. BsrV G263I overexpression with 6His C-terminal fusion (NcoI/NotI). The mutation was introduced with FCP132 and FCP133 primers, replacing G/I in BsrV 263 position.	This study
pET28b BsrV D268N	Kan^r. BsrV D268N overexpression with 6His C-terminal fusion (NcoI/NotI). The mutation was introduced with FCP157 and FCP158 primers, replacing D/N in BsrV 268 position.	This study
pET28b BsrV N348A	Kan^r. BsrV N348A overexpression with 6His C-terminal fusion (NcoI/NotI). The mutation was introduced with FCP134 and FCP135 primers, replacing N/A in BsrV 348 position.	This study
pET28b BsrV T349A	Kan^r. BsrV T349A overexpression with 6His C-terminal fusion (NcoI/NotI). The mutation was introduced with FCP136 and FCP137 primers, replacing T/A in BsrV 349 position.	This study
pET28b BsrV P391N	Kan^r. BsrV P391N overexpression with 6His C-terminal fusion (NcoI/NotI). The mutation was introduced with FCP138 and FCP40 primers, replacing P/N in BsrV 391 position.	This study
pET28b BsrV S377N	Kan^r. BsrV S377N overexpression with 6His C-terminal fusion (NcoI/NotI). The mutation was introduced with FCP139 primers, replacing S/N in BsrV 377 position.	This study
pET28b Bsr_{Ah}	Kan^r. BsrAh overexpression. 6His C-terminal fusion. (NcoI/HindIII). DNA fragment (*A. hydrofila*'s locus AHA2607) amplified with FCP345 and FCP388 primers.	This study

Supplementary Table S2. Primers used in this study.

NAME	SEQUENCE (5´→3´)
FCP37	aaaccatggagcagccgcttctcagtcgcaagaag
FCP38	catatcaatgccggccgcgcccatgccgccgtcattcagc
FCP40	ctagttattgctcagcggtg
FCP43	aaagcggccgctttcacgtagaaacgtgggttactggttcccc
FCP56	aaaccatggagcagccgcttctcagtcgcaagaag
FCP57	aaatctagatgccaaaggcgatctgtcgcagacgatgg
FCP58	gaattactcatcgtcaaatgcaggtccagcattggcgcagcagagagagagaaagaagg
FCP59	ccttctttctctctctctgctgcgccaatgctggacctgcatttgacgatgagtaattc
FCP60	ggtttctccaagttgtttgggtatagcctagtgatgatgatgatgatggccgctgctaacgcctgctccataataagacatttc
FCP61	gcagcggccatcatcatcatcatcactaggctatacccaaacaacttggagaaacc
FCP62	aaatctagatttactcttgagtcactttagtcggtg
FCP63	gcggatgtgtaattccgcagcagagag
FCP64	ctctctgctgcggaattacacatccgc
FCP106	aaatctagatgggtgaatggtggatgtg
FCP107	aaagaattccccaagaagatcaagcgct
FCP108	aaagaattccagtgtcttcttgtgcatg
FCP109	aaatctagagcccagcagatcaccatgc
FCP110	caccaaaattgccgccatcatg
FCP111	catgatggcggcaattttggtg
FCP112	gaactgatcgctgtgcgctctg
FCP113	cagagcgcacagcgatcagttc
FCP114	ccgtgtggcctctgccagcc
FCP115	ggctggcagaggccacacgg
FCP116	gttcacatcaagctgaatgac
FCP117	gtcattcagcttgatgtgaac
FCP118	catcgcgctggctgacggcggc
FCP119	gccgccgtcagccagcgcgatg
FCP120	ctgaatgacatcggcatgggcc
FCP121	ggcccatgccgatgtcattcag
FCP122	catgggccgtgccggcattg
FCP123	caatgccggcacggcccatg
FCP124	cccacttcaacaattacaatg
FCP125	cattgtaattgttgaagtggg
FCP126	cttcccgaatgccaatgcgg

FCP127	ccgcattggcattcgggaag
FCP128	gtgcgcgcagcactggctc
FCP129	gagccagtgctgcgcgcac
FCP130	gcgaactctgccaccgcgctc
FCP131	gagcgcggtggcagagttcgc
FCP132	cgtccaggtatcgtgttgtttg
FCP133	caaacaacacgatacctggacg
FCP134	catcgatggccaccactgtg
FCP135	cacagtggtggccatcgatg
FCP136	catcgatgaacgccactgtgg
FCP137	ccacagtggcgttcatcgatg
FCP138	caacgctgagctgattttcaatgag
FCP139	aaagcggccgctttcacgtagaaacgtgggttattggttc
FCP140	aaagcggccgcttagtgatgatgatgatgatggccgctgctggattggaagtacaggttctctttcacgtagaaacgtgggttactggttcccc
FCP157	gtgttgtttggtaatttgccaaccaaccc
FCP158	gggttggttggcaaattaccaaacaacac

Supplementary Table S3. Analysis of the bacterial species encoding BsrV-orthologues

Bacterial (specie)	Gram, class, family	Life style	Bsr-SP lengh* (aa)	Reference
Yersinia pseudotuberculosis	Gram -, ɣ -Proteobacteria, Enterobacteriaceae	Facultative pathogen	20	(Kaasch et al., 2012)
Yersinia pestis	Gram -, ɣ -Proteobacteria, Enterobacteriaceae	Facultative pathogen	20/21	(Williamson and Oyston, 2012)
Proteus mirabilis	Gram -, ɣ -Proteobacteria, Enterobacteriaceae	Facultative pathogen	20	(Jacobsen and Shirtliff, 2011)
Proteus penneri	Gram -, ɣ -Proteobacteria, Enterobacteriaceae	Facultative pathogen	20	(Rozalski et al., 2007)
***Citrobacter* sp.**	Gram -, ɣ -Proteobacteria, Enterobacteriaceae	Facult. pathogen	29	(Pepperell et al., 2002)
Providencia rustigianii	Gram -, ɣ -Proteobacteria, Enterobacteriaceae	Facultative pathogen	20	(O'Hara et al., 2000)
Providencia rettgeria	Gram -, ɣ -Proteobacteria, Enterobacteriaceae	Facultative pathogen	21	(O'Hara et al., 2000)
Providencia stuartii	Gram -, ɣ -Proteobacteria, Enterobacteriaceae	Facultative pathogen	24	(O'Hara et al., 2000)
Photobacterium profundum	Gram -, ɣ -Proteobacteria, Vibrionaceae	Environmental	21	(El-Hajj et al., 2010)
***Moritella* sp.**	Gram -, ɣ -Proteobacteria, Vibrionaceae	Environmental	25	(Delong et al., 1997)
Helicobacter hepaticus	Gram -, ε -Proteobacteria, Helicobacteraceae	Facultative pathogen	23	(Murakami, 2012)
Xenorhabdus bovienii	Gram -, ɣ -Proteobacteria, Enterobacteriaceae	Facultative pathogen	23	(Sugar et al., 2012)

Xenorhabdus nematophila	Gram -, ɣ -Proteobacteria, Enterobacteriaceae	Facultative pathogen	23	(Herbert and Goodrich-Blair, 2007)
Acinetobacter baumanii	Gram -, ɣ -Proteobacteria, Moraxellaceae	Facultative pathogen	28	(Howard et al., 2012)
Acinetobacter johnsoni	Gram -, ɣ -Proteobacteria, Moraxellaceae	Facultative pathogen	24	(Seifert et al., 1993)
Aeromonas hidrophyla	Gram -, ɣ -Proteobacteria, Aeromonadaceae	Facultative pathogen	22	(Chang et al., 1997)
Aeromonas salmonicida* subsp. *salmonicida	Gram -, ɣ -Proteobacteria, Aeromonadaceae	Facultative pathogen	22	(Romer Villumsen et al., 2012)
Kingella oralis	Gram -, β-Proteobacteria, Neisseriaceae	Facultative pathogen	24	(Chen, 1996)
Pseudomonas putida	Gram -, ɣ -Proteobacteria, Pseudomonadaceae	Facultative pathogen	24	(Kim et al., 2012)
Taylorella equigenitalis	Gram -, β-Proteobacteria,Alcaligenaceae	Facultative pathogen	23	(Timoney, 1996)
***Roseobacter* sp.**	Gram -, α-Proteobacteria, Rhodobacteraceae	Environmental	ND	(Lenk et al., 2012)
Vibrio cholerae	Gram -, ɣ -Proteobacteria, Vibrionaceae	Facultative pathogen	23/31	(Harris et al., 2012)
Vibrio parahaemoliticus	Gram -, ɣ -Proteobacteria, Vibrionaceae	Facultative pathogen	25	(Su and Liu, 2007)
Vibrio fischeri	Gram -, ɣ -Proteobacteria, Vibrionaceae	Facultative pathogen	20/21	(Su and Liu, 2007)
Vibrio furmisii	Gram -, ɣ -Proteobacteria, Vibrionaceae	Facultative pathogen	25	(Austin, 2010)
Vibrio mimicus	Gram -, ɣ -Proteobacteria, Vibrionaceae	Facultative pathogen	23	(Austin, 2010)
Vibrio caribbenthicus	Gram -, ɣ -Proteobacteria, Vibrionaceae	Environmental	23	(Austin, 2010)

Vibrio coralliilyticus	Gram -, ɣ -Proteobacteria, Vibrionaceae	Facultative pathogen	23	(Austin, 2010)
Vibrio metschnikovii	Gram -, ɣ -Proteobacteria, Vibrionaceae	Facultative pathogen	23	(Austin, 2010)
Shewanella halifaxensis	Gram -, ɣ -Proteobacteria, Shewanellaceae	Environmental	22	(Zhao et al., 2006)
***Reinekea* sp.**	Gram -, ɣ -Proteobacteria, Reinekea	Environmental	ND	(Pinhassi et al., 2007)

*Signal peptide length obtained with the SignalP 4.1 Server online tool. ND: Not determined

Supplementary Table S4. BsrV orthologs identified based on *in silico* comparative analysis.

BsrV orthologs
>gi|170024003|ref|YP_001720508.1| alanine racemase [Yersinia pseudotuberculosis YPIII]
>gi|169750537|gb|ACA68055.1| alanine racemase [Yersinia pseudotuberculosis YPIII]
>gi|186895776|ref|YP_001872888.1| alanine racemase [Yersinia pseudotuberculosis PB1/+]
>gi|186698802|gb|ACC89431.1| alanine racemase [Yersinia pseudotuberculosis PB1/+]
>gi|51596715|ref|YP_070906.1| alanine racemase [Yersinia pseudotuberculosis IP 32953]
>gi|51589997|emb|CAH21630.1| putative alanine racemase [Yersinia pseudotuberculosis IP 32953]
>gi|22125742|ref|NP_669165.1| alanine racemase [Yersinia pestis KIM 10]
>gi|108812106|ref|YP_647873.1| alanine racemase [Yersinia pestis Nepal516]
>gi|20137378|sp|Q8ZFL4.1|ALR2_YERPE RecName: Full=Alanine racemase 2
>gi|145599043|ref|YP_001163119.1| alanine racemase [Yersinia pestis Pestoides F]
>gi|149366357|ref|ZP_01888391.1| putative alanine racemase [Yersinia pestis CA88-4125]
>gi|153950742|ref|YP_001400629.1| alanine racemase [Yersinia pseudotuberculosis IP 31758]
>gi|165925439|ref|ZP_02221271.1| alanine racemase [Yersinia pestis biovar Orientalis str. F1991016]
>gi|165938444|ref|ZP_02227001.1| alanine racemase [Yersinia pestis biovar Orientalis str. IP275]
>gi|166008560|ref|ZP_02229458.1| alanine racemase [Yersinia pestis biovar Antiqua str. E1979001]
>gi|166210808|ref|ZP_02236843.1| alanine racemase [Yersinia pestis biovar Antiqua str. B42003004]
>gi|167422631|ref|ZP_02314384.1| alanine racemase [Yersinia pestis biovar Orientalis str. MG05-1020]
>gi|167426368|ref|ZP_02318121.1| alanine racemase [Yersinia pestis biovar Mediaevalis str. K1973002]
>gi|167468736|ref|ZP_02333440.1| alanine racemase [Yersinia pestis FV-1]
>gi|218928815|ref|YP_002346690.1| alanine racemase [Yersinia pestis CO92]
>gi|229841680|ref|ZP_04461838.1| putative alanine racemase [Yersinia pestis biovar Orientalis str. PEXU2]
>gi|229843797|ref|ZP_04463940.1| putative alanine racemase [Yersinia pestis biovar Orientalis str. India 195]
>gi|229894540|ref|ZP_04509722.1| putative alanine racemase [Yersinia pestis Pestoides A]
>gi|229902427|ref|ZP_04517546.1| putative alanine racemase [Yersinia pestis Nepal516]
>gi|270490394|ref|ZP_06207468.1| alanine racemase [Yersinia pestis KIM D27]
>gi|294504124|ref|YP_003568186.1| alanine racemase [Yersinia pestis Z176003]
>gi|21958663|gb|AAM85416.1|AE013788_2 putative alanine racemase [Yersinia pestis KIM 10]
>gi|108775754|gb|ABG18273.1| alanine racemase [Yersinia pestis Nepal516]
>gi|115347426|emb|CAL20330.1| putative alanine racemase [Yersinia pestis CO92]
>gi|145210739|gb|ABP40146.1| alanine racemase [Yersinia pestis Pestoides F]
>gi|149290731|gb|EDM40806.1| putative alanine racemase [Yersinia pestis CA88-4125]
>gi|152962237|gb|ABS49698.1| alanine racemase [Yersinia pseudotuberculosis IP 31758]
>gi|165913559|gb|EDR32179.1| alanine racemase [Yersinia pestis biovar Orientalis str. IP275]
>gi|165922548|gb|EDR39699.1| alanine racemase [Yersinia pestis biovar Orientalis str. F1991016]
>gi|165992942|gb|EDR45243.1| alanine racemase [Yersinia pestis biovar Antiqua str. E1979001]
>gi|166207988|gb|EDR52468.1| alanine racemase [Yersinia pestis biovar Antiqua str. B42003004]
>gi|166958478|gb|EDR55499.1| alanine racemase [Yersinia pestis biovar Orientalis str. MG05-1020]
>gi|167054723|gb|EDR64527.1| alanine racemase [Yersinia pestis biovar Mediaevalis str. K1973002]
>gi|229680473|gb|EEO76570.1| putative alanine racemase [Yersinia pestis Nepal516]
>gi|229689405|gb|EEO81468.1| putative alanine racemase [Yersinia pestis biovar Orientalis str. India 195]
>gi|229694143|gb|EEO84191.1| putative alanine racemase [Yersinia pestis biovar Orientalis str. PEXU2]
>gi|229703559|gb|EEO90576.1| putative alanine racemase [Yersinia pestis Pestoides A]
>gi|262362240|gb|ACY58961.1| alanine racemase [Yersinia pestis D106004]
>gi|262366174|gb|ACY62731.1| alanine racemase [Yersinia pestis D182038]
>gi|270338898|gb|EFA49675.1| alanine racemase [Yersinia pestis KIM D27]
>gi|294354583|gb|ADE64924.1| alanine racemase [Yersinia pestis Z176003]
>gi|320014832|gb|ADV98403.1| putative alanine racemase [Yersinia pestis biovar Medievalis str. Harbin 35]
>gi|108807830|ref|YP_651746.1| alanine racemase [Yersinia pestis Antiqua]
>gi|167401740|ref|ZP_02307231.1| alanine racemase [Yersinia pestis biovar Antiqua str. UG05-0454]
>gi|108779743|gb|ABG13801.1| putative alanine racemase [Yersinia pestis Antiqua]
>gi|167048845|gb|EDR60253.1| alanine racemase [Yersinia pestis biovar Antiqua str. UG05-0454]
>gi|237731612|ref|ZP_04562093.1| alanine racemase [Citrobacter sp. 30_2]
>gi|226907151|gb|EEH93069.1| alanine racemase [Citrobacter sp. 30_2]
>gi|226327902|ref|ZP_03803420.1| hypothetical protein PROPEN_01783 [Proteus penneri ATCC 35198]

>gi|225203606|gb|EEG85960.1| hypothetical protein PROPEN_01783 [Proteus penneri ATCC 35198]
>gi|197285632|ref|YP_002151504.1| alanine racemase [Proteus mirabilis HI4320]
>gi|194683119|emb|CAR43692.1| putative alanine racemase [Proteus mirabilis HI4320]
>gi|227356137|ref|ZP_03840526.1| alanine racemase [Proteus mirabilis ATCC 29906]
>gi|227163601|gb|EEI48517.1| alanine racemase [Proteus mirabilis ATCC 29906]
>gi|212710795|ref|ZP_03318923.1| hypothetical protein PROVALCAL_01863 [Providencia alcalifaciens DSM 30120]
>gi|212686492|gb|EEB46020.1| hypothetical protein PROVALCAL_01863 [Providencia alcalifaciens DSM 30120]
>gi|261345933|ref|ZP_05973577.1| alanine racemase [Providencia rustigianii DSM 4541]
>gi|282566018|gb|EFB71553.1| alanine racemase [Providencia rustigianii DSM 4541]
>gi|268589404|ref|ZP_06123625.1| alanine racemase [Providencia rettgeri DSM 1131]
>gi|291315242|gb|EFE55695.1| alanine racemase [Providencia rettgeri DSM 1131]
>gi|183599355|ref|ZP_02960848.1| hypothetical protein PROSTU_02822 [Providencia stuartii ATCC 25827]
>gi|188021591|gb|EDU59631.1| hypothetical protein PROSTU_02822 [Providencia stuartii ATCC 25827]
>gi|197334487|ref|YP_002155497.1| alanine racemase [Vibrio fischeri MJ11]
>gi|197315977|gb|ACH65424.1| alanine racemase [Vibrio fischeri MJ11]
>gi|59711342|ref|YP_204118.1| alanine racemase [Vibrio fischeri ES114]
>gi|59479443|gb|AAW85230.1| alanine racemase [Vibrio fischeri ES114]
>gi|54310452|ref|YP_131472.1| alanine racemase [Photobacterium profundum SS9]
>gi|46914893|emb|CAG21670.1| putative alanine racemase [Photobacterium profundum SS9]
>gi|153837983|ref|ZP_01990650.1| alanine racemase [Vibrio parahaemolyticus AQ3810]
>gi|149748591|gb|EDM59450.1| alanine racemase [Vibrio parahaemolyticus AQ3810]
>gi|28899622|ref|NP_799227.1| alanine racemase [Vibrio parahaemolyticus RIMD 2210633]
>gi|28807874|dbj|BAC61111.1| putative alanine racemase [Vibrio parahaemolyticus RIMD 2210633]
>gi|260364032|ref|ZP_05776760.1| alanine racemase [Vibrio parahaemolyticus K5030]
>gi|260876638|ref|ZP_05888993.1| alanine racemase [Vibrio parahaemolyticus AN-5034]
>gi|260898078|ref|ZP_05906574.1| alanine racemase [Vibrio parahaemolyticus Peru-466]
>gi|260902333|ref|ZP_05910728.1| alanine racemase [Vibrio parahaemolyticus AQ4037]
>gi|308085806|gb|EFO35501.1| alanine racemase [Vibrio parahaemolyticus Peru-466]
>gi|308093954|gb|EFO43649.1| alanine racemase [Vibrio parahaemolyticus AN-5034]
>gi|308110937|gb|EFO48477.1| alanine racemase [Vibrio parahaemolyticus AQ4037]
>gi|308114571|gb|EFO52111.1| alanine racemase [Vibrio parahaemolyticus K5030]
>gi|167624749|ref|YP_001675043.1| alanine racemase [Shewanella halifaxensis HAW-EB4]
>gi|167354771|gb|ABZ77384.1| alanine racemase [Shewanella halifaxensis HAW-EB4]
>gi|312882516|ref|ZP_07742257.1| alanine racemase [Vibrio caribbenthicus ATCC BAA-2122]
>gi|309369916|gb|EFP97427.1| alanine racemase [Vibrio caribbenthicus ATCC BAA-2122]
>gi|260778604|ref|ZP_05887496.1| alanine racemase [Vibrio coralliilyticus ATCC BAA-450]
>gi|260604768|gb|EEX31063.1| alanine racemase [Vibrio coralliilyticus ATCC BAA-450]
>gi|260772889|ref|ZP_05881805.1| alanine racemase [Vibrio metschnikovii CIP 69.14]
>gi|260612028|gb|EEX37231.1| alanine racemase [Vibrio metschnikovii CIP 69.14]
>gi|149910818|ref|ZP_01899452.1| alanine racemase [Moritella sp. PE36]
>gi|149806152|gb|EDM66132.1| alanine racemase [Moritella sp. PE36]
>gi|54303604|ref|YP_133597.1| alanine racemase [Photobacterium profundum SS9]
>gi|46917035|emb|CAG23797.1| putative alanine racemase [Photobacterium profundum SS9]
>gi|27366912|ref|NP_762439.1| alanine racemase [Vibrio vulnificus CMCP6]
>gi|34098524|sp|Q8D6Q0.1|ALR2_VIBVU RecName: Full=Alanine racemase 2
>gi|27358479|gb|AAO07429.1| alanine racemase [Vibrio vulnificus CMCP6]
>gi|37676689|ref|NP_937085.1| alanine racemase [Vibrio vulnificus YJ016]
>gi|37201232|dbj|BAC97055.1| alanine racemase [Vibrio vulnificus YJ016]
>gi|320158793|ref|YP_004191171.1| alanine racemase [Vibrio vulnificus MO6-24/O]
>gi|319934105|gb|ADV88968.1| alanine racemase [Vibrio vulnificus MO6-24/O]
>gi|161582006|ref|NP_230956.2| alanine racemase [Vibrio cholerae O1 biovar El Tor str. N16961]
>gi|255745708|ref|ZP_05419656.1| alanine racemase [Vibrio cholera CIRS 101]
>gi|262159017|ref|ZP_06030129.1| alanine racemase [Vibrio cholerae INDRE 91/1]
>gi|262169374|ref|ZP_06037066.1| alanine racemase [Vibrio cholerae RC27]
>gi|255736783|gb|EET92180.1| alanine racemase [Vibrio cholera CIRS 101]
>gi|262022187|gb|EEY40896.1| alanine racemase [Vibrio cholerae RC27]
>gi|262029202|gb|EEY47854.1| alanine racemase [Vibrio cholerae INDRE 91/1]
>gi|121586566|ref|ZP_01676352.1| alanine racemase, putative [Vibrio cholerae 2740-80]
>gi|121726850|ref|ZP_01680062.1| alanine racemase, putative [Vibrio cholerae V52]

>gi|147673980|ref|YP_001216876.1| alanine racemase [Vibrio cholerae O395]
>gi|153819283|ref|ZP_01971950.1| alanine racemase, putative [Vibrio cholerae NCTC 8457]
>gi|153822911|ref|ZP_01975578.1| alanine racemase, putative [Vibrio cholerae B33]
>gi|227081483|ref|YP_002810034.1| alanine racemase, putative [Vibrio cholerae M66-2]
>gi|229505102|ref|ZP_04394612.1| alanine racemase [Vibrio cholerae BX 330286]
>gi|229511228|ref|ZP_04400707.1| alanine racemase [Vibrio cholerae B33]
>gi|229518346|ref|ZP_04407790.1| alanine racemase [Vibrio cholerae RC9]
>gi|229608106|ref|YP_002878754.1| alanine racemase [Vibrio cholerae MJ-1236]
>gi|254848434|ref|ZP_05237784.1| alanine racemase [Vibrio cholerae MO10]
>gi|298498598|ref|ZP_07008405.1| alanine racemase [Vibrio cholerae MAK 757]
>gi|9655801|gb|AAF94470.1| alanine racemase, putative [Vibrio cholerae O1 biovar El Tor str. N16961]
>gi|121549245|gb|EAX59277.1| alanine racemase, putative [Vibrio cholerae 2740-80]
>gi|121630754|gb|EAX63139.1| alanine racemase, putative [Vibrio cholerae V52]
>gi|126510186|gb|EAZ72780.1| alanine racemase, putative [Vibrio cholerae NCTC 8457]
>gi|126519563|gb|EAZ76786.1| alanine racemase, putative [Vibrio cholerae B33]
>gi|146315863|gb|ABQ20402.1| putative alanine racemase [Vibrio cholerae O395]
>gi|227009371|gb|ACP05583.1| alanine racemase, putative [Vibrio cholerae M66-2]
>gi|227013229|gb|ACP09439.1| alanine racemase, putative [Vibrio cholerae O395]
>gi|229345061|gb|EEO10035.1| alanine racemase [Vibrio cholerae RC9]
>gi|229351193|gb|EEO16134.1| alanine racemase [Vibrio cholerae B33]
>gi|229357325|gb|EEO22242.1| alanine racemase [Vibrio cholerae BX 330286]
>gi|229370761|gb|ACQ61184.1| alanine racemase [Vibrio cholerae MJ-1236]
>gi|254844139|gb|EET22553.1| alanine racemase [Vibrio cholerae MO10]
>gi|297542931|gb|EFH78981.1| alanine racemase [Vibrio cholerae MAK 757]
>gi|20137517|sp|Q9KSE5.2|ALR2_VIBCH RecName: Full=Alanine racemase 2
>gi|254226880|ref|ZP_04920449.1| alanine racemase [Vibrio cholerae V51]
>gi|125620597|gb|EAZ48962.1| alanine racemase [Vibrio cholerae V51]
>gi|297578895|ref|ZP_06940823.1| conserved hypothetical protein [Vibrio cholerae RC385]
>gi|297536489|gb|EFH75322.1| conserved hypothetical protein [Vibrio cholerae RC385]
>gi|262190944|ref|ZP_06049158.1| alanine racemase [Vibrio cholerae CT 5369-93]
>gi|262033181|gb|EEY51705.1| alanine racemase [Vibrio cholerae CT 5369-93]
>gi|153216974|ref|ZP_01950738.1| alanine racemase, putative [Vibrio cholerae 1587]
>gi|124114006|gb|EAY32826.1| alanine racemase, putative [Vibrio cholerae 1587]
>gi|229515688|ref|ZP_04405147.1| alanine racemase [Vibrio cholerae TMA 21]
>gi|229347457|gb|EEO12417.1| alanine racemase [Vibrio cholerae TMA 21]
>gi|254286591|ref|ZP_04961547.1| alanine racemase, putative [Vibrio cholerae AM-19226]
>gi|150423349|gb|EDN15294.1| alanine racemase, putative [Vibrio cholerae AM-19226]
>gi|153802661|ref|ZP_01957247.1| alanine racemase, putative [Vibrio cholerae MZO-3]
>gi|124121789|gb|EAY40532.1| alanine racemase, putative [Vibrio cholerae MZO-3]
>gi|229521424|ref|ZP_04410843.1| alanine racemase [Vibrio cholerae TM 11079-80]
>gi|229341522|gb|EEO06525.1| alanine racemase [Vibrio cholerae TM 11079-80]
>gi|153830040|ref|ZP_01982707.1| putative alanine racemase [Vibrio cholerae 623-39]
>gi|148874480|gb|EDL72615.1| putative alanine racemase [Vibrio cholerae 623-39]
>gi|153827222|ref|ZP_01979889.1| alanine racemase, putative [Vibrio cholerae MZO-2]
>gi|149738872|gb|EDM53204.1| alanine racemase, putative [Vibrio cholerae MZO-2]
> gi|229525903|ref|ZP_04415308.1| alanine racemase [Vibrio cholerae bv. albensis VL426]
>gi|229339484|gb|EEO04501.1| alanine racemase [Vibrio cholerae bv. albensis VL426]
>gi|229529606|ref|ZP_04418996.1| alanine racemase [Vibrio cholerae 12129(1)]
>gi|229333380|gb|EEN98866.1| alanine racemase [Vibrio cholerae 12129(1)]
>gi|261210961|ref|ZP_05925251.1| alanine racemase [Vibrio sp. RC341]
>gi|260839936|gb|EEX66536.1| alanine racemase [Vibrio sp. RC341]
>gi|262402336|ref|ZP_06078897.1| alanine racemase [Vibrio sp. RC586]
>gi|262351118|gb|EEZ00251.1| alanine racemase [Vibrio sp. RC586]
>gi|262165566|ref|ZP_06033303.1| alanine racemase [Vibrio mimicus VM223]
>gi|262025282|gb|EEY43950.1| alanine racemase [Vibrio mimicus VM223]
>gi|262171654|ref|ZP_06039332.1| alanine racemase [Vibrio mimicus MB-451]
>gi|261892730|gb|EEY38716.1| alanine racemase [Vibrio mimicus MB-451]
>gi|258621589|ref|ZP_05716622.1| Alanine racemase [Vibrio mimicus VM573]
>gi|258586207|gb|EEW10923.1| Alanine racemase [Vibrio mimicus VM573]
>gi|258627600|ref|ZP_05722377.1| Alanine racemase [Vibrio mimicus VM603]
>gi|258580182|gb|EEW05154.1| Alanine racemase [Vibrio mimicus VM603]

>gi|315181783|gb|ADT88696.1| alanine racemase [Vibrio furnissii NCTC 11218]
>gi|260769245|ref|ZP_05878178.1| alanine racemase [Vibrio furnissii CIP 102972]
>gi|260614583|gb|EEX39769.1| alanine racemase [Vibrio furnissii CIP 102972]
>gi|28900856|ref|NP_800511.1| alanine racemase [Vibrio parahaemolyticus RIMD 2210633]
>gi|260362532|ref|ZP_05775452.1| alanine racemase [Vibrio parahaemolyticus K5030]
>gi|260879223|ref|ZP_05891578.1| alanine racemase [Vibrio parahaemolyticus AN-5034]
>gi|260896758|ref|ZP_05905254.1| alanine racemase [Vibrio parahaemolyticus Peru-466]
>gi|34098472|sp|Q87HG4.1|ALR2_VIBPA RecName: Full=Alanine racemase 2
>gi|28809302|dbj|BAC62344.1| putative alanine racemase [Vibrio parahaemolyticus RIMD 2210633]
>gi|308087318|gb|EFO37013.1| alanine racemase [Vibrio parahaemolyticus Peru-466]
>gi|308094088|gb|EFO43783.1| alanine racemase [Vibrio parahaemolyticus AN-5034]
>gi|308115278|gb|EFO52818.1| alanine racemase [Vibrio parahaemolyticus K5030]
>gi|153836908|ref|ZP_01989575.1| alanine racemase [Vibrio parahaemolyticus AQ3810]
>gi|149749866|gb|EDM60611.1| alanine racemase [Vibrio parahaemolyticus AQ3810]
>gi|260901465|ref|ZP_05909860.1| alanine racemase [Vibrio parahaemolyticus AQ4037]
>gi|308107691|gb|EFO45231.1| alanine racemase [Vibrio parahaemolyticus AQ4037]
>gi|262395354|ref|YP_003287207.1| alanine racemase [Vibrio sp. Ex25]
>gi|262338948|gb|ACY52742.1| alanine racemase [Vibrio sp. Ex25]
>gi|91224603|ref|ZP_01259864.1| alanine racemase [Vibrio alginolyticus 12G01]
>gi|91190491|gb|EAS76759.1| alanine racemase [Vibrio alginolyticus 12G01]
>gi|32265965|ref|NP_859997.1| alanine racemase [Helicobacter hepaticus ATCC 51449]
>gi|32262014|gb|AAP77063.1| alanine racemase [Helicobacter hepaticus ATCC 51449]
>gi|290476786|ref|YP_003469697.1| Alanine racemase 2 [Xenorhabdus bovienii SS-2004]
>gi|289176130|emb|CBJ82935.1| Alanine racemase 2 [Xenorhabdus bovienii SS-2004]
>gi|300724984|ref|YP_003714309.1| putative alanine racemase [Xenorhabdus nematophila ATCC 19061]
>gi|297631526|emb|CBJ92233.1| putative alanine racemase [Xenorhabdus nematophila ATCC 19061]
>gi|262368964|ref|ZP_06062293.1| alanine racemase [Acinetobacter johnsonii SH046]
>gi|262316642|gb|EEY97680.1| alanine racemase [Acinetobacter johnsonii SH046]
>gi|293608485|ref|ZP_06690788.1| conserved hypothetical protein [Acinetobacter sp. SH024]
>gi|292829058|gb|EFF87420.1| conserved hypothetical protein [Acinetobacter sp. SH024]
>gi|193077032|gb|ABO11785.2| alanine racemase [Acinetobacter baumannii ATCC 17978]
>gi|126641403|ref|YP_001084387.1| alanine racemase [Acinetobacter baumannii ATCC 17978]
>gi|145298692|ref|YP_001141533.1| alanine racemase [Aeromonas salmonicida subsp. salmonicida A449]
>gi|142851464|gb|ABO89785.1| alanine racemase [Aeromonas salmonicida subsp. salmonicida A449]
>gi|117619060|ref|YP_857116.1| alanine racemase [Aeromonas hydrophila subsp. hydrophila ATCC 7966]
>gi|117560467|gb|ABK37415.1| alanine racemase [Aeromonas hydrophila subsp. hydrophila ATCC 7966]
>gi|238022778|ref|ZP_04603204.1| hypothetical protein GCWU000324_02689 [Kingella oralis ATCC 51147]
>gi|237865981|gb|EEP67117.1| hypothetical protein GCWU000324_02689 [Kingella oralis ATCC 51147]
>gi|223939404|ref|ZP_03631282.1| alanine racemase [bacterium Ellin514]
>gi|223891896|gb|EEF58379.1| alanine racemase [bacterium Ellin514]
>gi|319779710|ref|YP_004130623.1| Alanine racemase [Taylorella equigenitalis MCE9]
>gi|317109734|gb|ADU92480.1| Alanine racemase [Taylorella equigenitalis MCE9]
>gi|73763191|gb|AAZ83975.1| alanine racemase [Pseudomonas putida]
>gi|167033190|ref|YP_001668421.1| alanine racemase [Pseudomonas putida GB-1]
>gi|166859678|gb|ABY98085.1| alanine racemase [Pseudomonas putida GB-1]
>gi|313498322|gb|ADR59688.1| Alr [Pseudomonas putida BIRD-1]
>gi|26990430|ref|NP_745855.1| alanine racemase [Pseudomonas putida KT2440]
>gi|24985399|gb|AAN69319.1|AE016569_3 alanine racemase, putative [Pseudomonas putida KT2440]
>gi|148547263|ref|YP_001267365.1| alanine racemase [Pseudomonas putida F1]
>gi|148511321|gb|ABQ78181.1| alanine racemase [Pseudomonas putida F1]
>gi|86138387|ref|ZP_01056961.1| alanine racemase [Roseobacter sp. MED193]
>gi|85824912|gb|EAQ45113.1| alanine racemase [Roseobacter sp. MED193]
>gi|88800370|ref|ZP_01115936.1| alanine racemase [Reinekea sp. MED297]
>gi|88776947|gb|EAR08156.1| alanine racemase [Reinekea sp. MED297]

Supplementary Materials and Methods

Growth conditions. All *V. cholerae* strains used in this study were derived from the sequenced El Tor clinical isolate N16961 (Heidelberg et al., 2000). *E. coli* and *V. cholerae* were grown in Luria broth (LB), on LB agar plates or in minimal medium (Na_2HPO_4-$7H_2O$ 64 g/L, KH_2PO_4 15 g/L, NH_4Cl 5 g/L, NaCl 2.5 g/L per liter of distilled water) supplemented with glucose 0.2% at 37ºC. Antibiotics were used at the following concentrations (per ml): 200 µg streptomycin (Sm); 50 µg ampicillin (Ap) or carbenicillin (Cb) and 50 µg kanamycin (Kn) (*V. cholerae*).

DNA amplification and cloning. Plasmids and primers are listed in Tables S1 and S2. DNA was amplified using 1 $U.ml^{-1}$ of DNA polimerase from *Pyrococcus furiosus* (Roche Molecular Biochemicals) in its recommended buffer with $MgCl_2$ 3 mM, dNTP mixture 0.5 mM and 50 pmol of each primer (Sigma-Aldrich). When required, overlap extension techniques were used following appropriate protocols (Nelson and Fitch, 2011).

Bacterial transformation. *E. coli* competence was induced following Inoue's method (Inoue et al., 1990). The transformation was carried out following the method described by Hanahan (Hanahan, 1985).

Protein expression and purification. The *V. cholerae* genes encoding wt and mutant BsrV, and AlrV, Alr_{Ah} and Bsr_{Ah} were cloned in pET28b (Novagen) for expression in *E. coli* BL21(DE3) cells (Rosenberg et al., 1987). Expression was induced (at OD_{600}=0.4) with 1 mM IPTG for 3 h. Cell pellets were resuspended in 50 mM Tris HCl pH 7.2, 150 mM NaCl, 10% glycerol, and Complete Protease Inhibitor Cocktail Tablets (Roche), and lysed with 3 passes through a French press. Proteins were purified from cleared lysates (30 min, 50,000 rpm) on Ni-NTA agarose columns (Qiagen), and eluted with a

discontinuous imidazol gradient. Pure proteins were visualized by SDS-PAGE electrophoretic protein separation (Laemmli and Favre, 1973). N-terminal sequence revealed that BsrV and Bsr_{Ah} were purified as the predicted full length mature proteins: BsrV (residues 24-407); Bsr_{Ah} (residues 22-408). Untagged BsrV was purified from its His-tagged derivative (see Table S2) which presents a Tobacco etch virus (TEV) protease protease cleavage site preceding the His-tag. TEV protease (Sigma) digestion was performed at 30°C for 6h, in 25 mM Tris-HCl, pH 8.0, 150 - 500 mM NaCl, 14 mM β-mercaptoethanol.

Racemase activity assays. All racemase assays were done in 2 fundamental steps. First, the mixture was prepared in a 50 μl final volume with: Tris-HCl 50 mM pH 8, L-amino acid at various concentrations, and 0.47 μM of racemase (AlrV, BsrV, ΔCl-BsrV, Bsr_{Ah} and all single BsrV-mutants in the SDP signature residues). All amino acids used as substrate were purchased from Sigma Aldrich (St. Louis, MO). The reaction was performed for 5 minutes (steady-state kinetics) or 90 minutes (long term assay). Then reactions were stopped by boiling during 10 min and samples were spin for 10 minutes at 14,500 rpm to remove inactivated proteins. Next, D-amino acid production was determined by coupling 10 μl of the extract into 150 μl of a reaction containing: sodium phosphate buffer 100 mM pH 7, *Trigonopsis variabilis* D-amino acid oxidase (DAAO) (Komarova et al., 2012) 3.6 U/ml, horseradish peroxidase 1 U/ml, o-phenilendiamine (OPD) 2 mg/ml and FAD 3 mg/ml. This two step assay permits the quantification of H_2O_2 (DAAO is able to produce α-ketoacid, NH_3 and H_2O_2 from DAA). Peroxidase reduces H_2O_2 releasing free O_2 that reacts with OPD, leading to the production of 2,3-

diaminophenazine. The reaction was incubated for 2 hours at 37ºC and inactivated with HCl 3 M, giving a colorimetric product that can be measured at 492 nm.

For those cases where DAAO activity was a constrain (i.e. His, Cys), or for competition assays, Marfey's (FDAA)-derivatization of L- and D-forms of amino acids and HPLC analysis was followed (described below).

The kinetic parameters were determined by measuring production rates for different substrate concentrations (1.25 – 60 mM) of each L-amino acid with 0.47 μM racemase. The activities for each substrate concentration were measured thrice. All mean activities were plotted and adjusted to a Michaelis–Menten model to determine the apparent K_m, V_{max}, and k_{cat} by non-linear regression (Microsoft Office 2007 and Solver macro) (De Levie, 2001). k_{cat} was determined as $V_{max}/[E_0]$, where $[E_0]$ = nmol of racemase/ml. Reaction kinetics for His and Cys were not established given that L-His is not a DAAO substrate and L-Cys is a peroxidase inhibitor. The ε used to determine the kinetic parameters was 1,220 m/cm and the molecular weight of the enzyme monomer without signal peptide used to determine the k_{cat} was 42 kDa.

Marfey-derivatized amino acids analysis. The product from a racemization reaction was derivatized with L-FDAA (1-fluoro-2-4-dinitrophenyl-5-L-alanine amide, Marfey's reagent, Thermo Scientific). First, an equal volume of $NaHCO_3$ 0.5 M was added to the racemization reaction; then, 6 µl of this reaction was reacted with FDAA (10 mg/ml in acetone) at 80ºC for 3 min. The reaction was stopped with HCl 2N and the samples were filtered. The products were separated with a linear gradient of triethylamine phosphate/acetonitrile in HPLC with an Aeris peptide column (250 x 4.6 mm; 3.6 µm particle size) (Phenomenex, USA) and detected at Abs.340 nm.

Crystallization of BsrV, ΔCl-BsrV, Bsr_{Ah} and Alr_{Ah}. High-throughput techniques using a NanoDrop™ ExtY robot (Innovadyne Technologies Inc.) were carried out to test initial crystallization assays based on commercial Qiagen® screenings, JCSG+Suite™ and PACT™ Suite, and Hampton Research® screenings, IINDEX™ and Crystal Screen™ 1 and 2. All crystallization nano-trials were performed by sitting-drop vapour-diffusion method at 291 K using Innovaplate™ SD-2 microplates (Innovadyne Technologies Inc.) and mixing equal amounts (250 nl) of purified aliquots of BsrV (4.5 mg/ml and 3.0 mg/ml, both in 20 mM Tris, pH 7.0), BsrV-RN/AA (ΔCl-BsrV) (6.25 mg/ml and 3.5 mg/ml, both in 20 mM Tris pH 7.0), Bsr_{Ah} (8 mg/ml in 20 mM Tris pH 7.0), Alr_{Ah} (6 mg/ml in 20 mM Tris–HCl pH 7.5) and precipitant solutions. NanoDrop robot drops (500 nl, protein and precipitant solutions) were equilibrated against 65 ml of mother liquor. BsrV rhomboid microcrystals grew from several conditions of INDEX™, PACT™ Suite and JCSG+Suite™. The conditions were systematically improved, and finally, the best quality crystals grew in the condition composed by 0.1 M Bis-Tris propane pH 7.5, 0.2 M Sodium Iodide, and 20% (p/v) of PEG 3350. These crystals were obtained using the sitting drop method (1:1 volume proportion), mixing 2 µl of wt BsrV (holoenzyme) at 3.0 mg/ml with 1 µl of precipitant solution, and equilibrated against 500 µl of mother liquor. Good quality crystals from purified ΔCl-BsrV (3.5 mg/ml in Tris pH 7.0) were obtained in the improved condition constituted by 0.1 M Bis-Tris Propane pH 7.5, 0.2 M Sodium Bromide and 29% PEG 3,350. Bsr_{Ah} microcrystals grew from JCSG+Suite™ condition number 77 (5mM CoCl2, 5mM $CdCl_2$, 5mM $MgCl_2$, 5mM $NiCl_2$, 0.1M Hepes pH 7.5 and 12% PEG 3350). The Bsr_{Ah} crystallization condition was scaled to a 3 µl drop (precipitant/protein ratio 2:1) and finally improved to obtain good quality diffracting

crystals at the condition composed by 5 mM CoCl2, 5 mM CdCl2, 5 mM MgCl2, 5 mM NiCl2, 0.1 M Hepes pH 7.5 and 16% PEG 3350. Alr_{Ah} microcrystals grew from the PACT™ Suite condition number 63 (0.1 M Bis Tris propane pH 6.5, 0.2 M Sodium iodide, 20% PEG 3350). Various additives and detergents (Hampton Research) were tested around these conditions, but none of them led to improvement of the crystals size and/or diffraction quality. The final condition (0.1 M Bis Tris propane pH 6.5, 0.2 M Sodium iodide, 14% PEG 3350) was scaled to bigger drops (2 µl).

X-ray data collection and structural determination. Holoenzyme and ΔCl-BsrV crystals of BsrV were soaked for 5 s in a cryoprotectant solution (15% v/v of glycerol diluted in crystallization mother liquor) prior to flash-cooling at 100 K in liquid nitrogen. X-ray data sets up to 1.1 Å resolution were collected using synchrotron radiation facility at the beamline ID29 (ESRF, Grenoble) for the holoenzyme and several data sets up to 1.5 Å for the ΔCl-BsrV crystals at the X06SA beamline (SLS, Villigen). Both holoenzyme and ΔCl-BsrV data sets were collected at 100 K using a PILATUS 6M detector (holoenzyme: oscillation range 0.1º, ΔCl-BsrV: oscillation range 0.25º). All data sets were processed using XDS (Kabsch, 1993) and scaled using SCALA (Evans, 2006) from CCP4 program suite. Data processing results are summarized in Table 1. BsrV structure was solved by molecular replacement method (MR) with the program MolRep from CCP4 program suite using the *E. coli* alanine racemace (PDB code 2RJG) as template. The structural model was refined with the PHENIX program (Adams et al., 2010) and manually improved using COOT (Emsley and Cowtan, 2004). The final models for both holoenzyme and ΔCl-BsrV presented good stereochemistry. Crystals of Alr_{Ah} were soaked for 5 s in a cryoprotectant solution (15% v/v of glycerol diluted in

crystallization mother liquor) prior to flash-cooling at 100 K in liquid nitrogen. X-ray data sets up to 1.4 Å resolution were collected using synchrotron radiation facility at the beamline ID14-4 (ESRF, Grenoble) using an ADSC Q315r detector (oscillation range 1º), and processed (results are sumarized in Table 1) using XDS (Kabsch, 1993) and scaled using SCALA (Evans, 2006) from CCP4 program suite. Bsr_{Ah} structure was solved by MR method with the program MolRep from CCP4 program suite using BsrV structure as template. The structural model of Bsr_{Ah} was refined with the PHENIX program (Adams et al., 2010) and manually improved using COOT (Emsley and Cowtan, 2004). Crystals of Alr_{Bs} were cryoprotected by a quick soak in 0.1 M Bis Tris propane pH 6.5, 0.2 M Sodium iodide, 14% PEG 3350, 15% glicerol. X-ray diffraction were collected at the ID29 beamline (ESRF, Grenoble) using a PILATUS 6M detector (oscillation range 0.1º). Although several X-ray data collections were measured, the maximum resolution reached was 3.25 Å. Diffraction data were processed (results are sumarized in Table 1) using XDS (Kabsch, 1993) and scaled using SCALA (Evans, 2006) from CCP4 program suite. The crystal structure of Alr_{Ah} was solved by MR method, using the BALBES program (Long et al., 2008). A very incomplete initial model was obtained (<50% of the residues in the AU were correctly positioned, R-factor 47%) and subsequently, the main chain was fixed in density using strict geometry restrains and the incomplete regions were traced manually in COOT (Emsley and Cowtan, 2004). adding alanines as first attempt. Due to the low resolution, during this process the alanine racemase structure from *Pseudomonas aeruginosa* (PDB code 1RCQ) was used as template. The structure was refined using BUSTER-TNT program (Bricogne, 2011) with NCS, TLS, and automatic low resolution restrains. The B-factors were

refined as groups. Several cycles of refinement and manual model rebuilding were necessary to reach a good model, which included four independent proteins of 357 amino acids. The waters molecules were assigned with BUSTER-TNT. The refinement statistics are summarized in Table 1. The stereochemistry of the models was verified with MOLPROBITY (Chen et al., 2009).

Identification of new putative broad-spectrum racemases and the residues responsible for the substrate specificity

The initial retrieval or PLP-racemases sequences for studying the subfamily structure was performed by searching with BLAST (Altschul et al., 1997), using AlrV as query sequence, against a non-redundant protein database, with a restrictive E-value cutoff of $1e^{-10}$. This search resulted in 2,967 sequences, which included BsrV. Protein sequences not present in the dataset due to the redundancy filter for which experimental or structural information regarding substrate specificity was available were added, including alanine racemases from *E. coli, V. cholerae* and *A. hydrophila*. The resulting sequences were filtered selecting only those mapped into the UniProt database, yielding a preliminary set of 1,355 protein sequences.

The protein dataset was aligned using the multiple sequence alignment tool MUSCLE6 (v3.8.31). The resulting MSA was filtered out for empty columns and for redundant proteins (using a 95% redundancy threshold) using the Jalview7 tool (v2.7), resulting in 137 sequences in the final MSA used for inferring the PLP-racemase subfamily composition and associated “specificity determining positions” (SDPs).

Identification of SDPs was carried out using the Xdet and S3Det programs implemented in the JDet package. JDet allows extracting, visualizing and manipulating fully

conserved positions and family dependent positions in MSAs3. S3Det not only detects SDPs but also defines the subfamily composition of the MSA2.

A phylogenetic tree was constructed from the same MSA to compare it with the partition of the MSA into subfamilies generated by S3Det. The tree was based on the neighbor joining method using substitution matrix BLOSUM62 and was built using the Jalview7 tool (v2.7). The manipulation and display of the resulting phylogenetic tree was carried out with iTool8.

After this initial filtered alignment was used for predicting the structure of the PLP-racemase family and the associated SDPs, a comprehensive search and classification of this family of proteins was carried out. Using AlrV and BsrV as query sequences, two BLAST searches were carried out (E-value cutoff $1e^{-5}$) yielding a final joint set of 2,540 sequences. The two searches converged virtually to the same set of sequences. These sequences were aligned with MUSCLE (Edgar, 2004) and S3Det was used to infer the subfamily composition of the resulting MSA. The resulting subfamilies were assigned to AlrV-like or BsrV-like ("specific" and "broad") depending on their "enrichment" in the sequences previously classified (in the MSA of 137 sequences). Consequently, a subfamily of 1,800 sequences containing 68 out of the 84 AlrV-like (and only 1 out of the 11 BsrV-like) was assigned to the "specific" class. The proteins within a cluster of 74 sequences containing 10 out of the 11 BsrV-like (and no AlrV-like) were consequently assigned as putative new BsrV-like.

Supplementary references

Adams, P.D., Afonine, P.V., Bunkoczi, G., Chen, V.B., Davis, I.W., Echols, N., Headd, J.J., Hung, L.W., Kapral, G.J., Grosse-Kunstleve, R.W*., et al.* (2010). Acta Crystallogr D Biol Crystallogr *66*, 213-221.

Altschul, S.F., Madden, T.L., Schaffer, A.A., Zhang, J., Zhang, Z., Miller, W., and Lipman, D.J. (1997). Nucleic Acids Res *25*, 3389-3402.

Austin, B. (2010). Vet Microbiol *140*, 310-317.

Bricogne, G.B.E., Brandl, M., Flensburg, C., Keller, P., Paciorek, W., et al. (2011). BUSTER version X.Y.Z. Cambridge, United Kingdom: Global Phasing Ltd.

Chang, C.Y., Thompson, H., Rodman, N., Bylander, J., and Thomas, J. (1997). Ann Clin Lab Sci *27*, 254-259.

Chen, C. (1996). Oral Microbiol Immunol *11*, 425-427.

Chen, Y., Zhang, W., Shi, Q., Hesek, D., Lee, M., Mobashery, S., and Shoichet, B.K. (2009). J Am Chem Soc *131*, 14345-14354.

De Levie, R. (2001). How to Use Excel in Analytical Chemistry and in General Scientific Data Analysis. . Cambridge Univ Press, Cambridge.

Delong, E.F., Franks, D.G., and Yayanos, A.A. (1997). Appl Environ Microbiol *63*, 2105-2108.

Edgar, R.C. (2004). Nucleic Acids Res *32*, 1792-1797.

El-Hajj, Z.W., Allcock, D., Tryfona, T., Lauro, F.M., Sawyer, L., Bartlett, D.H., and Ferguson, G.P. (2010). Ann N Y Acad Sci *1189*, 143-148.

Emsley, P., and Cowtan, K. (2004). Acta Crystallogr D Biol Crystallogr *60*, 2126-2132.

Evans, P. (2006). Acta Crystallogr D Biol Crystallogr *62*, 72-82.

Hanahan, D. (1985). DNA cloning: A Practical Approach IRL Press, Oxford, United Kingdom *vol. 1*, 109-135.

Harris, J.B., LaRocque, R.C., Qadri, F., Ryan, E.T., and Calderwood, S.B. (2012). Lancet *379*, 2466-2476.

Heidelberg, J.F., Eisen, J.A., Nelson, W.C., Clayton, R.A., Gwinn, M.L., Dodson, R.J., Haft, D.H., Hickey, E.K., Peterson, J.D., Umayam, L*., et al.* (2000).. Nature *406*, 477-483.

Herbert, E.E., and Goodrich-Blair, H. (2007). Nat Rev Microbiol *5*, 634-646.

Howard, A., O'Donoghue, M., Feeney, A., and Sleator, R.D. (2012). Virulence *3*, 243-250.

Inoue, H., Nojima, H., and Okayama, H. (1990). Gene *96*, 23-28.

Jacobsen, S.M., and Shirtliff, M.E. (2011). Virulence *2*, 460-465.

Kaasch, A.J., Dinter, J., Goeser, T., Plum, G., and Seifert, H. (2012). Infection *40*, 185-190.

Kabsch, W. (1993). J Appl Cryst *26*, 795-800.

Kim, S.E., Park, S.H., Park, H.B., Park, K.H., Kim, S.H., Jung, S.I., Shin, J.H., Jang, H.C., and Kang, S.J. (2012). Chonnam Med J *48*, 91-95.

Komarova, N.V., Golubev, I.V., Khoronenkova, S.V., Chubar, T.A., and Tishkov, V.I. (2012). Biochemistry (Mosc) *77*, 1181-1189.

Laemmli, U.K., and Favre, M. (1973). J Mol Biol *80*, 575-599.

Lam, H., Oh, D.C., Cava, F., Takacs, C.N., Clardy, J., de Pedro, M.A., and Waldor, M.K. (2009). Science *325*, 1552-1555.
Lenk, S., Moraru, C., Hahnke, S., Arnds, J., Richter, M., Kube, M., Reinhardt, R., Brinkhoff, T., Harder, J., Amann, R.*, et al.* (2012). ISME J *6*, 2178-2187.
Long, F., Vagin, A.A., Young, P., and Murshudov, G.N. (2008). Acta Crystallogr D Biol Crystallogr *64*, 125-132.
Murakami, K. (2012). J Gastroenterol *47*, 724-725.
Nelson, M.D., and Fitch, D.H. (2011). Methods Mol Biol *772*, 459-470.
O'Hara, C.M., Brenner, F.W., and Miller, J.M. (2000). Clin Microbiol Rev *13*, 534-546.
Pepperell, C., Kus, J.V., Gardam, M.A., Humar, A., and Burrows, L.L. (2002). Antimicrob Agents Chemother *46*, 3555-3560.
Pinhassi, J., Pujalte, M.J., Macian, M.C., Lekunberri, I., Gonzalez, J.M., Pedros-Alio, C., and Arahal, D.R. (2007). Int J Syst Evol Microbiol *57*, 2370-2375.
Romer Villumsen, K., Dalsgaard, I., Holten-Andersen, L., and Raida, M.K. (2012). PLoS One *7*, e46733.
Rosenberg, A.H., Lade, B.N., Chui, D.S., Lin, S.W., Dunn, J.J., and Studier, F.W. (1987). Gene *56*, 125-135.
Rozalski, A., Kwil, I., Torzewska, A., Baranowska, M., and Staczek, P. (2007). Postepy Hig Med Dosw (Online) *61*, 204-219.
Seifert, H., Strate, A., Schulze, A., and Pulverer, G. (1993). Clin Infect Dis *17*, 632-636.
Su, Y.C., and Liu, C. (2007). Food Microbiol *24*, 549-558.
Sugar, D.R., Murfin, K.E., Chaston, J.M., Andersen, A.W., Richards, G.R., deLeon, L., Baum, J.A., Clinton, W.P., Forst, S., Goldman, B.S.*, et al.* (2012) Environ Microbiol *14*, 924-939.
Timoney, P.J. (1996). Comp Immunol Microbiol Infect Dis *19*, 199-204.
Williamson, E.D., and Oyston, P.C. (2012). J Med Microbiol *61*, 911-918.
Zhao, J.S., Manno, D., Leggiadro, C., O'Neil, D., and Hawari, J. (2006). Int J Syst Evol Microbiol *56*, 205-212.